

Large-angle elastic scattering of 59.54-keV photons by elements with $12 \leq Z \leq 92$

J. S. Shahi,¹ Sanjiv Puri,² D. Mehta,³ M. L. Garg,⁴ Nirmal Singh,¹ and P. N. Trehan¹

¹*Department of Physics, Panjab University, Chandigarh-160 014, India*

²*Department of Physics, SLIET, Longowal-148 106, India*

³*Department of Physics and Astrophysics, Delhi University, Delhi-110 007, India*

⁴*Department of Biophysics, Panjab University, Chandigarh-160 014, India*

(Received 13 January 1998)

Elastic-scattering cross sections for 59.54-keV photons have been measured at an angle of 121° for 42 elements in the atomic region $12 \leq Z \leq 92$. The measurements were performed using a ^{241}Am radioisotope as the photon source and a Si (Li) detector. The measured cross sections have been compared with those based on the modified-relativistic form factors (MF's), a combination of the MF's and angle-independent "anomalous" scattering factors (MF+ASF), and the relativistic second-order S -matrix calculations. The MF cross sections are found to be enormously higher for the elements with K -shell binding energy (E_K) close to the incident photon energy (E_{inc}) of 59.54 keV. The S matrix and MF+ASF cross sections, in general, represent the trend of the measured data over the whole atomic region under investigation. These theoretical cross sections are in good agreement with the measured data for the elements with $12 \leq Z \leq 26$ and, thereafter, deviate with increasing Z . The S matrix and MF+ASF values are, on the average, higher by 17%, and 24%, respectively, for the elements with $39 \leq Z \leq 67$; and by 10% and 19%, respectively, for the elements with $70 \leq Z \leq 92$. In case of ^{68}Er , having a K -shell binding energy 2.1 keV lower than the incident photon energy, the MF+ASF value shows good agreement with the measured one, and the S matrix value is lower by 12%.

[S1050-2947(98)08405-4]

PACS number(s): 32.80.Cy

I. INTRODUCTION

The elastic scattering of photons, being one of the fundamental modes of their interaction with matter, has been a subject of substantial theoretical and experimental interest. The elastic scattering of low-energy photons (soft-x-ray regime) by atoms is mainly contributed by scattering from the bound atomic electrons, i.e., the Rayleigh scattering process. The scattering contribution from the nucleus and the quantum electrodynamics effects are significant only at higher photon energies. The elastic scattering of photons by atoms, molecules, and solids is an important method of obtaining information about structural properties of materials [1,2]. The comparison of the elastic scattering by a complex system, e.g., macromolecules, with that by the free constituent atoms, can provide information about the structure of the complex system [2]. Accurate data regarding the elastic-scattering cross sections is required for an evaluation of narrow-beam photon attenuation coefficients [1] and dosimetric computations for medical physics and reactor physics [3,4]. The knowledge of elastic and inelastic scattering of x-ray photons is also useful in different ways for the quantitative elemental analysis using energy dispersive x-ray fluorescence (EDXRF) technique [5].

Different theoretical approaches have been developed to evaluate the Rayleigh scattering cross sections. The two major basic approaches are (i) a form-factor formalism [6–8], which was developed as correction factor to the well-known Thomson formula for scattering off a classical point electron charge by an extended charge distribution; and (ii) a numerical partial-wave solution of elastic-scattering amplitudes for the second-order S -matrix element in a central potential [9–11]. A recent review of the elastic-scattering cross-section

calculations, based on these approaches, was given in Refs. [12,13]. Extensive tabulations of form factors based on different calculations are available in literature [6–8]. Nonrelativistic [6] and relativistic [7] form factors are based on calculations involving nonrelativistic and relativistic individual electron and total atom wave functions. The modified-relativistic form factor (MF) [8] is an improved version of the relativistic form factor, and takes into account the correction due to electron binding. Further, in the case of elastic scattering of photons with energy in the vicinity of the electron binding energy of the interacting atom, corrections are included to account for the effects related to atomic structure, such as virtual excitation and ionization of atomic electrons. These corrections to the modified relativistic form factors are commonly known as anomalous scattering factors (ASF's) [14,15]. Extensive tabulations of ASF's are available in the literature [14–17]. The magnitude of this correction, which is generally taken to be angle independent, becomes quite significant (i) for elements with electron binding energies close to the incident photon energy, and (ii) at large (backward) scattering angles where the MF cross sections become much smaller as compared to those at forward angles. The second-order S -matrix approach provides a better calculation of elastic scattering than is normally available from simpler, form-factor approaches. The cross-section data based on second-order S -matrix formalism, for all the elements in the atomic region $1 \leq Z \leq 103$ and in the energy range 0.0543–2754.1 keV, recently became available from Kissel [17].

In the present work, elastic-scattering cross sections for 59.54-keV photons have been measured at an angle of 121° (corresponding to a momentum transfer at 4.17 \AA^{-1}) for 42 elements in the atomic region $12 \leq Z \leq 92$. The measurements were carried out using a ^{241}Am radioisotope as the photon

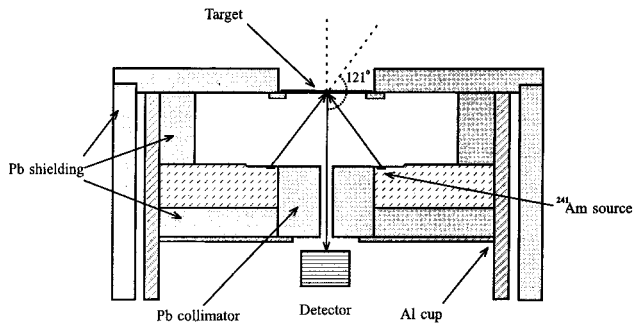


FIG. 1. Target, source, and detector geometrical arrangement used for the present measurements.

source in the annular geometry, suitable for scattering measurements at large angles. These cross sections have been compared with those based on the modified-relativistic form factors a combination of the MF's and anomalous scattering factors (MF+ASF), and the relativistic second-order S -matrix calculations (S -mat.). The present work covers the atomic region $12 \leq Z \leq 92$ thoroughly, with an emphasis on the elements (around $Z=70$) having a K -shell binding energy in proximity to the incident photon energy. The elastic-scattering cross-section measurements for such cases at large angles are expected to provide a stringent test of the current theoretical understanding.

Earlier measurements [18–26] of the elastic scattering of 59.54-keV photons included a limited number of elements for a vividly wide range of Z , and exhibited inconsistencies in certain cases. The scattering cross sections for Al, Cu, Mo, Yb, Ta, Au, and Pb at an angle of 141° , measured by Varier and Unnikrishnan [22], and for Al, V, Mo, Cd, and Pb at 60° , 90° , and 120° , measured by Casnati, Baraldi, and Tartari [23], show good agreement with the S -matrix calculations. Ghose *et al.* [24] found the measured cross sections for Er and Yb to be lower, by up to 15%, than the S -matrix and MF+ASF values at backward angles, and in good agreement at forward angles. Nayak *et al.* [25] measured the elastic-scattering cross sections at 90° for 13 elements with $29 \leq Z \leq 92$, and the results were found to be lower by up to 20% than the S -matrix values in case of Cd and Mo, and even double in case of Yb. We reported elastic-scattering measurements [26] at an angle of 130° for 19 elements in the atomic region $13 \leq Z \leq 82$; out of these, 14 elements were taken in the atomic region $13 \leq Z \leq 50$. The measured values are found to be higher than the S -matrix calculations by up to 20%. All previous measured results [18–26] showed large deviations from the MF-based cross sections for the elements with a K -shell binding energy close to 59.54 keV.

II. EXPERIMENTAL DETAILS

A. Experimental procedure

The geometrical arrangement, shown in Fig. 1, is similar to the one used for our earlier measurements at 22.1-keV photon energy [27]. It consisted of the exciter system NER-496 (New England Nuclear, U.S.) and an annular source of ^{241}Am (300 mCi, procured from DUPONT, U.S.). The source is in the form of a circular flat ribbon of 30-mm diameter and 4-mm width. The 59.54-keV γ -ray photons,

emitted from the ^{241}Am source (emission probability is 35.6 per 100 decays [28]), were made to scatter from different targets through an angle of 121° . A Si (Li) detector ($28.27 \text{ mm}^2 \times 5.5 \text{ mm}$, and full widths at half maximum 180 eV at 5.89 keV and 400 eV at 59.54 keV), with a 3-mm-diameter Pb collimator, was used to detect the scattered and fluorescent radiations from the target. The W-alloy shield, supplied with the exciter system NER-496, was replaced by the Pb shield to avoid the W $K\alpha_1$ x-ray peak in the background spectrum (Fig. 2 of Ref. [26]), which overlaps with the 59.54-keV elastic-scattered peak. The exciter system and detector were kept in a Pb housing. The whole arrangement resulted in smooth background in the region of the elastic scattered peak [Fig. 2(a)].

Spectroscopically pure, self-supporting foils of Mg, Al, Si, Ti, V, Fe, Ni, Cu, Zn, Ge, Y, Zr, Nb, Mo, Rh, Pd, Ag, Cd, In, Sn, Gd, Tb, Dy, Ho, Er, Yb, Ta, W, Re, Pt, Ir, Au, and Pb, mounted on perspex rings of 1-in. diameter, were used as targets. The thickness of these foils were in the range 8–430 mg/cm^2 . Self-supporting pellets (thickness 300–1000 mg/cm^2) of S, Ru, Sb, and Te (metallic powder); barium carbonate [$\text{Ba}(\text{CO}_3)$], bismuth oxycarbonate ($\text{Bi}_2\text{O}_2\text{CO}_3$), thorium nitrate [$\text{Th}(\text{NO}_3)_4$], and uranyl acetate [$\text{UO}_2(\text{CH}_3\text{COO})_2 \cdot 2\text{H}_2\text{O}$] were also used. The Hg target was prepared by sealing liquid mercury between two layers of 10- μm -thick mylar.

The spectra were taken using a PC-based multichannel analyzer (Canberra, Model S-100). To reduce the statistical error in measurements, three spectra were recorded for time intervals ranging from 3 to 10 h. In the case of the low- Z targets, the recording time for each spectrum was 25 h. Further, to minimize systematic errors, different spectra for each target were taken on different occasions. Two or more targets of different thickness have been used for some of the elements. In all the measurements, the total count rate in the detector was less than 200 cps. This ensured the stability of the system, and avoided deterioration of spectrum due to random summing effects. Further, in the case of In, Sn, Sb, and Te, the peaks corresponding to random summing of the intense K x rays lie in the region of the elastic-scattered peak. The measurements for these elements were done by placing the Cu absorber (thickness of 250 mg/cm^2) at the collimator-end close to the Si (Li) detector. This arrangement reduced the K x-ray count rate considerably, thereby resulting in negligible summing effects. Measurements for most of the targets were repeated using an experimental setup with a 5-mm-diameter Pb collimator in front of the detector.

Typical spectra from Er and W targets are shown in Figs. 2(b) and 2(c). It is clear from these spectra that the elastic and inelastic-scattered γ -ray peaks are well resolved. The energy shift of the inelastic scattered peak from the elastic scattered peak in spectrum of the low- Z targets was used to deduce the scattering angle (121°). The centroid of the inelastic-scattered peak was determined from the spectrum corrected channelwise for the efficiency of the detector. Further, computer-based simulations were used to estimate the angular spread of the detected scattered photons, i.e., to determine the number of elastic-scattered photons, reaching the detector, as a function of scattering angle. Figure 3 depicts simulated results for the present experimental setup, with 3 and 5-mm-diameter detector collimators.

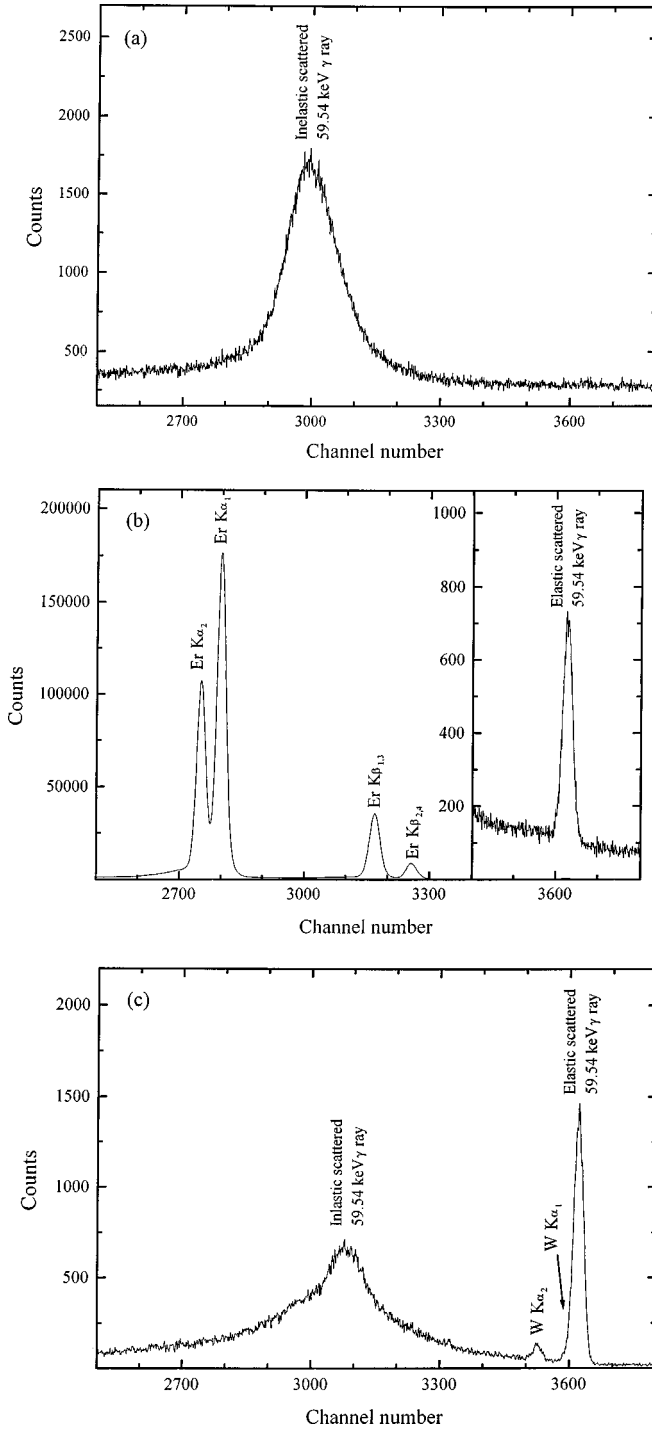


FIG. 2. (a) Background spectrum with no target placed at its position, (b) and (c) Typical spectra of 59.54-keV photons scattered through an angle of 121° by Er target (63.7 mg/cm^2), and by W target (97.4 mg/cm^2), respectively.

B. Evaluation procedure

The measured differential cross sections for the elastic scattering of 59.54-keV photons were evaluated using the relation

$$\left(\frac{d\sigma}{d\Omega}\right)_{\text{el}} = \frac{N_{\text{el}}}{4\pi I_0 G \varepsilon_{\text{el}} m \beta}, \quad (1)$$

where N_{el} is the number of counts/s under the elastic scat-

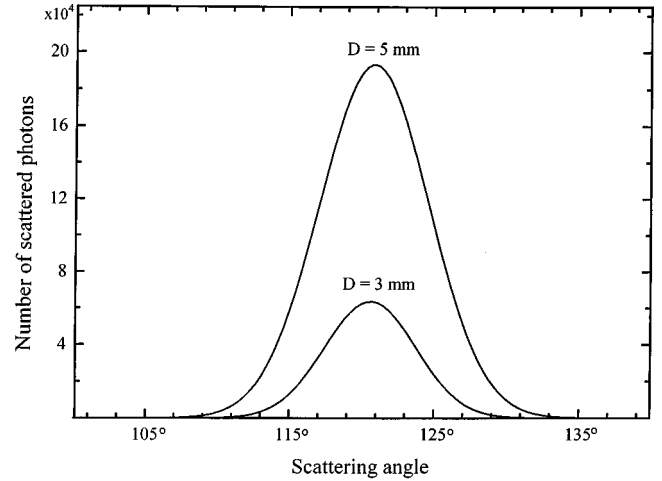


FIG. 3. Computer-simulated intensity profile for the elastic scattered photons reaching the detector as a function of scattering angle. D is the diameter of the Pb collimator in front of the detector.

tered peak, $I_0 G$ is the intensity of 59.54-keV photons falling on the portion of target visible to the detector, ε_{el} is the detector efficiency at 59.54 keV, m is thickness of the target foil in g/cm^2 , and β is the absorption correction factor which accounts for absorption of the incident and the elastic scattered photons in target. The value of β has been calculated using the procedure given in our earlier paper [27].

To determine number of counts/s under the elastic scattered peak, N_{el} , each spectrum was analyzed for photopeak areas corresponding to the elastic scattered photons using a computer code PEAKFIT [27,29]. In the spectra of Yb and W targets, the contribution of Yb- $K\beta_{1,3}$ and W- $K\alpha_1$ x rays (excited by the high energy γ rays emitted from the ^{241}Am source [28]) to the elastic scattered 59.54 keV peak, was estimated from the well-separated Yb- $K\beta_{2,4}$ and W- $K\alpha_2$ x ray peaks [Fig. 2(b)] and by using their relative intensities [30]. This contribution was 5% and 14% in Yb and W targets, respectively.

The product $I_0 G \varepsilon_{\text{el}}$ corresponding to the 59.54-keV photons emitted from the ^{241}Am annular source was determined, in the same geometrical arrangement (with 5- as well as 3-mm-diameter detector collimators) as used for the scattering measurements, using the following procedure. The set of $I_0 G \varepsilon$ values (set A) was determined over the energy range 24–50 keV, by taking $K\alpha$ x-ray spectra from spectroscopically pure targets of In, Sn, BaF_2 , PrF_3 , NdF_3 , SmF_3 , EuF_3 , TbF_3 , GdF_3 , DyF_3 , HoF_3 , ErF_3 , and TmF_3 (thickness 100–300 $\mu\text{g/cm}^2$, Micromatter, U.S.) with mylar backing, excited by the 59.54-keV photons emitted from the ^{241}Am source and by using the expression

$$I_0 G \varepsilon = \frac{N_{K\alpha}}{\sigma_{K\alpha} \beta m} \quad (2)$$

where $\sigma_{K\alpha}$ is the $K\alpha$ x-ray fluorescence cross section, and was taken from Ref. [31]. Other symbols have same meaning as explained above for Eq. (1), but now these correspond to $K\alpha$ x rays. Another set of $I_0 G \varepsilon$ values (set B) over the energy range 10–50 keV was generated using the targets Ge, Se, Sr, Y, Nb, Mo, Rh, and Pd (thickness 100–300 $\mu\text{g/cm}^2$),

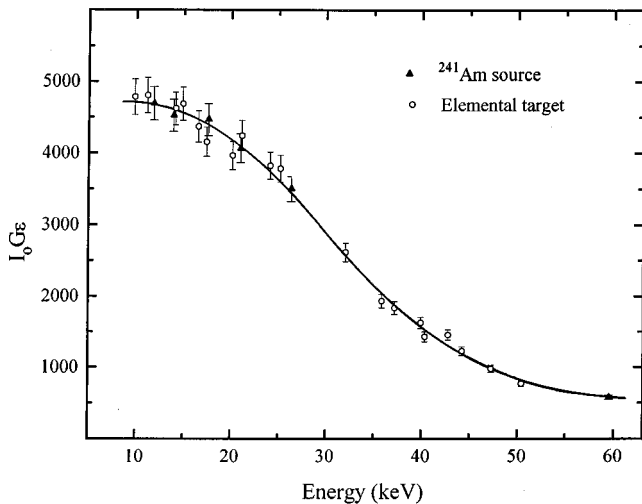


FIG. 4. Plot of $I_0 G \epsilon$ vs the detected photon energy.

in addition to those used for generating set A. For these measurements, the ^{241}Am annular source was covered with Cu-Al graded absorber (880-mg/cm²-thick Cu and 550-mg/cm²-thick Al) to absorb the 26.34-keV γ ray and Np L x rays, and thus acted as a 59.54-keV monochromatic source. This set of $I_0 G \epsilon$ values was normalized to set A. The normalized set was further extended to 59.54 keV by using relative efficiency values of the Si Li detector at energies corresponding to the 26.34- and 59.54-keV γ rays and the Np-Li ($i = \alpha, \beta, \gamma$) x rays, determined by using the ^{241}Am calibration source. Finally, the $I_0 G \epsilon$ value at 59.54 keV was used in Eq. (1). The $I_0 G \epsilon$ values, obtained using a 3-mm-diameter detector collimator, are shown as a function of energy in Fig. 4. It may be mentioned that the contribution to the production of target $K\alpha$ x rays due to high-energy photons (γ rays and bremsstrahlung) from the ^{241}Am exciter source [28], is estimated to be less than 1%.

III. RESULTS AND DISCUSSIONS

The present measured cross sections for elastic scattering of 59.54-keV photons at an angle of 121° by 42 elements in the atomic region $12 \leq Z \leq 92$ are listed in Table I. The errors in the measured cross sections are estimated to be 6–8%, and are attributed to the uncertainties in different parameters used in Eq. (1), namely, evaluation of photopeak areas (2%), the absorption coefficients used to evaluate β (4%), target thickness (2–4%) and the evaluation of the $I_0 G \epsilon_{\text{el}}$ factor (4%). The error in the uniformity of targets is taken to be negligible in case of thick targets with $\beta \leq 0.21$.¹ In these thick targets, error in the product $m\beta$ [used in Eq. (1)] is due to the absorption coefficients only. The scattering cross sections for an element, measured by using targets of different thicknesses, are found to agree within experimental errors (Table II). The weighted average of the results obtained us-

¹A value of $\beta = 0.21$ corresponds to 99% absorption. Below this value of β , the product $m\beta$ can be safely taken as constant equal to $[m(\mu_1/\cos\theta + \mu_2)^{-1}]$ (the limiting value of the product $m\beta$ when $m \rightarrow \infty$) [27].

ing targets of different thicknesses has been taken, including all the above-mentioned errors, except that in the $I_0 G \epsilon_{\text{el}}$ factor. The error in the $I_0 G \epsilon_{\text{el}}$ value was added in quadrature to that evaluated in the weighted average result. In the case of elements, where the measurements were done using 3 as well as 5-mm-diameter detector collimators, the results are found to agree well, and their average value is included in Table I. It is worth mentioning that the earlier measured scattering cross sections [18–25] have been reported relative to the form-factor-based inelastic-scattering cross section of a low- Z element like Al or Be, which was used in a determination of the incident photon intensity and other geometrical factors. In the present work, more reliable K x-ray fluorescence cross sections, having no angular dependence, have been used to evaluate the $I_0 G \epsilon$ factor. In the case of Ba, Bi, Th, and U, thick targets of their compounds (Table I) were used for the elastic-scattering cross-section measurements. The other elements present in the compound targets, being of low Z , contribute negligibly (<1%) to the elastic scattering as compared to the element of interest. It may be mentioned that ^{69}Tm , with a K -shell binding energy ($E_K = 59.39$ keV) very close to the incident photon energy, poses difficulties in a measurement of the elastic-scattering cross section because of the overlap of the strong Tm $K\beta_{2,4}$ x-ray peak with the elastic-scattered peak. In this case, the $K\beta_{2,4}$ x-ray fluorescence cross section, $\sigma_{K\beta_{2,4}} = 9.45$ b/sr [30,31], is considerably larger than the theoretically predicted elastic-scattering cross sections, $\sigma_{\text{el}} = 0.51$ b/sr [17], at 121°. Efforts are being made to measure the elastic-scattering cross section for the ^{69}Tm element.

The present measured elastic-scattering cross sections are compared, in Table I, with those evaluated using the form-factor approaches, namely, MF, MF+ASF, and the second-order S -matrix formalism. The percentage deviations of calculated cross sections from measured values are also given in this table. In calculations of the MF-based cross sections, the modified-relativistic form factors, $g(q)$, tabulated by Schaupp *et al.* [8], have been used in Eq. (4) of Ref. [27]. The cross sections based on MF's, including the angle-independent ASF's and the S -matrix calculations, have been taken from Kissel [17]. These calculations were performed using the same relativistic potential, i.e., the relativistic Hartree-Fock-Slater potential with the Latter tail. It is noteworthy that the theoretical elastic-scattering cross sections for different elements exhibit only a small angular dependence at back angles (Fig. 5). The average theoretical cross sections for different elements, evaluated by taking the weighted average of cross sections at various scattering angles in proportion to the number of scattered photons (Fig. 3), were found to be higher than the theoretical values at 121° by less than 1.5%. The theoretical scattering cross sections at 121° have been used as such in Table I for comparison with the measured values.

The measured and theoretical elastic-scattering cross sections are plotted in Fig. 6 as a function of atomic number (Z) of the scattering element. The MF values are, in general, lower than the measured values for low- and medium- Z elements (below $Z = 56$), and then the trend reverses for higher- Z elements. The deviations become enormously large in case of ^{70}Yb and then decrease with increasing Z . The MF values

TABLE I. Elastic-scattering cross sections for the 59.54-keV photons at an angle of 121°.

Element (Z)	K-shell binding energy (keV)	Scattering cross sections (mb/sr)			Percentage deviations from experimental cross sections			
		Experimental	MF+ASF	Calculated <i>S</i> -mat.	MF	MF+ASF	<i>S</i> -mat.	MF
Mg (12)	1.305	6.53(39)	6.90	6.84	6.31	6	5	-3
Al (13)	1.560	9.92(60)	9.99	9.88	9.13	1	0	-8
Si (14)	1.839	13.3(8)	13.7	13.5	12.5	3	2	-6
S (16)	2.472	20.2(16)	22.6	22.3	20.6	12	10	2
Ti (22)	4.965	53.1(32)	54.6	52.8	47.6	3	-1	-10
V (23)	5.465	60.0(36)	60.1	57.9	51.8	0	-3	-14
Fe (26)	7.112	73.2(51)	77.7	74.0	64.1	6	1	-12
Ni (28)	8.332	85.6(51)	91.7	86.8	73.4	7	1	-14
Cu (29)	8.981	87.1(52)	99.8	94.2	78.7	15	8	-10
Zn (30)	9.569	95.5(60)	109	102	84.6	14	7	-12
Ge (32)	11.104	118(8)	131	123	92.1	11	4	-22
Y (39)	17.038	222(15)	271	252	192	22	14	-14
Zr (40)	17.998	248(15)	300	280	212	21	13	-14
Nb (41)	18.986	262(18)	332	311	234	27	19	-10
Mo (42)	20.000	302(18)	367	343	258	21	13	-15
Ru (44)	22.117	370(26)	442	414	311	19	12	-16
Rh (45)	23.200	379(23)	483	452	340	27	19	-10
Pd (46)	24.350	438(30)	525	492	370	20	13	-15
Ag (47)	25.514	482(34)	564	533	401	17	11	-17
Cd (48)	26.711	498(30)	613	575	434	22	15	-13
In (49)	27.940	528(36)	658	617	467	25	17	-12
Sn (50)	29.200	575(39)	704	660	500	22	15	-13
Sb (51)	30.491	580(41)	749	702	534	29	21	-8
Te (52)	31.813	588(42)	793	743	568	34	26	-3
Ba (56) ^a	37.441	720(52)	952	894	698	32	24	-3
Gd (64)	50.329	845(59)	1087	1024	926	29	21	10
Tb (65)	51.996	856(60)	1071	1010	954	25	18	11
Dy (66)	53.788	861(61)	1036	968	983	20	12	14
Ho (67)	55.618	772(54)	967	902	1012	26	18	32
Er (68)	57.486	885(70)	845	781	1043	-4	-12	18
Yb (70)	61.332	280(24)	334	317	1109	19	13	296
Ta (73)	67.416	647(39)	745	689	1223	15	6	89
W (74)	69.525	712(51)	838	783	1266	18	10	78
Re (75)	71.676	796(55)	932	862	1312	17	9	65
Ir (77)	76.111	982(67)	1118	1029	1416	14	5	44
Pt (78)	78.395	1010(62)	1214	1116	1473	20	10	46
Au (79)	80.725	1089(79)	1312	1204	1534	20	11	41
Hg (80)	83.103	1162(74)	1415	1296	1600	22	12	38
Pb (82)	88.004	1360(85)	1633	1492	1746	20	10	28
Bi (83) ^a	90.526	1450(104)	1750	1596	1825	21	10	26
Th (90) ^a	109.651	2280(165)	2716	2469	2512	19	8	10
U (92) ^a	115.606	2376(176)	3028	2751	2737	27	16	15

^aSelf-supporting pellets of Ba(CO)₃, Bi₂O₂CO₃, Th(NO₃)₄, and UO₂(CH₃COO)₂ · 2H₂O were used in case of Ba, Bi, Th, and U, respectively.

after correction for ASF's and the *S*-matrix values, in general, represent the trend of the measured data over the whole atomic region under investigation. Both these sets of theoretical cross sections match well for low-*Z* elements, and the difference increases slowly up to 10% for high-*Z* elements. It may be mentioned that differences of the MF+ASF cross sections from the *S*-matrix values have been predicted to increase with an increasing momentum-transfer parameter [17].

The comparison of theoretical and measured cross sections is better presented in Fig. 7 by plotting their ratios as a function of *Z*. The MF values are in agreement with the measured values for the elements with $Z \leq 16$, and are, on the average, lower by 14% for the elements with $22 \leq Z \leq 50$. Thereafter, the deviations decrease up to $Z = 56$, and, further for the elements with $64 \leq Z \leq 92$, the MF values are higher than the measured ones. The deviations are considerably larger for elements having a *K*-shell binding energy (also

TABLE II. Measured elastic-scattering cross sections (mb/sr) for the 59.54-keV photons using targets of different thickness.

Element	Thickness (mg/cm ²)	Absorption correction (β)	Scattering cross sections
Mo (42)	71.4	0.664	300(20)
	122.3	0.515	304(21)
	193.7	0.379	302(23)
Cd (48)	54.3	0.647	502(33)
	182.9	0.301	494(35)
Ta (74)	51.5	0.785	640(43)
	430.4	0.234	654(45)
Pt (78)	37.4	0.806	990(66)
	258.3	0.308	1020(70)
Pb (82)	65.2	0.658	1340(92)
	184.0	0.361	1390(95)

included in Table I) in proximity to the incident photon energy. In the case of ${}_{70}\text{Yb}$ with $E_K/E_{\text{inc}} = 1.03$, the MF cross section is even ~ 4 times the measured value, and, thereafter, the deviations decrease with increasing E_K/E_{inc} . In the case of ${}_{90}\text{Th}$ and ${}_{92}\text{U}$ with $E_K/E_{\text{inc}} \sim 2$, the deviations reduce to $\sim 12\%$. The S matrix and MF+ASF values are, on the average, higher by 11% and 18%, respectively, than the measured ones. Both these sets show good agreement with the measured data for the elements with $Z \leq 26$, having a K -shell binding energy well below the incident photon energy ($E_K/E_{\text{inc}} < 0.12$). Furthermore, these theoretical values start to deviate with increasing Z , and exhibit nearly constant deviations over the atomic region $39 \leq Z \leq 67$. The S matrix and MF+ASF values are, on the average, higher than the measured values by 17% and 24%, respectively, in this atomic region. In the case of ${}_{68}\text{Er}$, with a K -shell binding energy 2.1 keV lower than the incident photon energy, the MF+ASF value shows good agreement with the measured one, and the S -matrix value is lower by 12%. For the elements with $70 \leq Z \leq 92$, the S -matrix values are, on the average, higher by

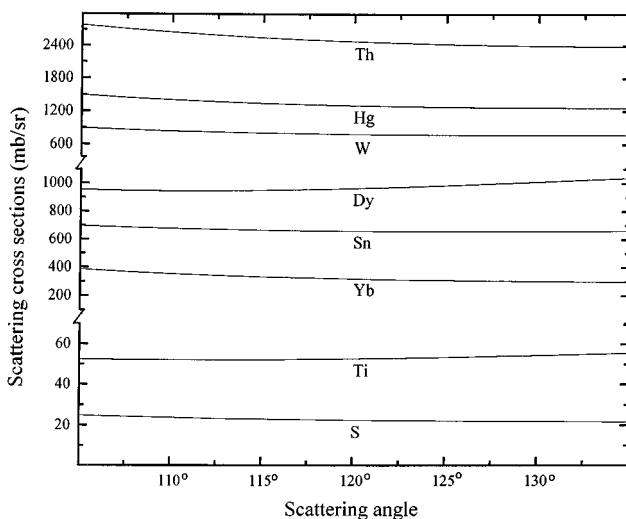


FIG. 5. Elastic scattering cross sections for 59.54-keV photons based on the S -matrix calculations [17] as a function of scattering angle.

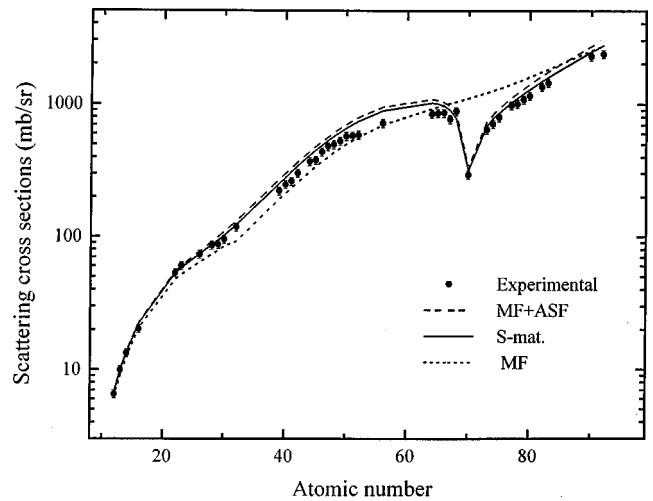


FIG. 6. Differential cross sections (mb/sr) for elastic scattering as a function of atomic number.

10% than the measured values, while the MF+ASF values are higher by 19%. The deviations of MF+ASF cross sections from the measured data exhibit an increasing trend in this atomic region. This trend is possibly due to the increasing significance of the L_1 -subshell binding energies as compared to the incident photon energy. The E_{L_1}/E_{inc} values increases from 0.20 to 0.36 over the atomic region $70 \leq Z \leq 92$. The elements with $Z = 32-42$, having E_K/E_{inc} values in this range, exhibit similar deviations. Similar observations have been reported by us from the elastic-scattering cross-section measurements at 117° for 22.1-keV photons in the atomic region $12 \leq Z \leq 92$ [27]. In this work, the MF+ASF and the S -matrix cross sections are found to be, on the average, higher by $\sim 10\%$ than the measured values. The deviations increase up to 20% in the case of elements with K -shell and L_1 -subshell binding energies just below the incident photon energy, and further decrease to $\sim 5\%$ in the case of elements

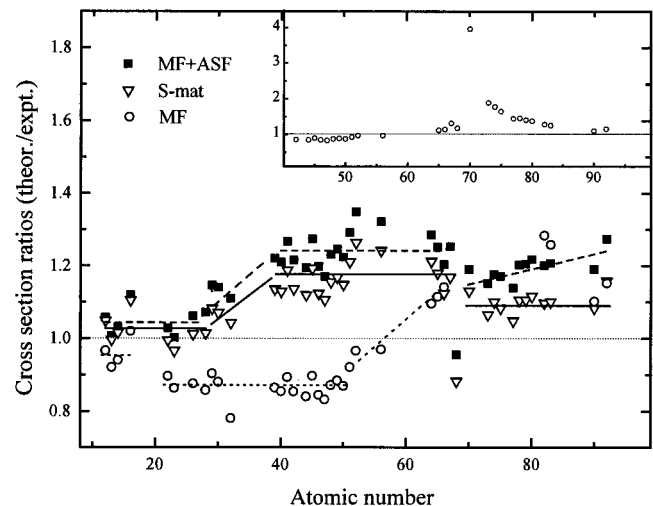


FIG. 7. Elastic-scattering cross-section ratios $\sigma(\text{theor.})/\sigma(\text{expt.})$, as a function of atomic number. The dotted, dashed, and solid lines are drawn to guide the eye and correspond to $\sigma(\text{MF})/\sigma(\text{expt.})$, $\sigma(\text{MF+ASF})/\sigma(\text{expt.})$ and $\sigma(\text{S-mat.})/\sigma(\text{expt.})$ values, respectively. The part of the plot, where the $\sigma(\text{MF})/\sigma(\text{expt.})$ values are large, is shown in the inset.

with a K -shell binding energy above the incident photon energy. The measured cross sections for Al and Mg, having electron binding energies far below the incident photon energy, show good agreement with the MF, MF+ASF and S -matrix values. The elastic-scattering cross sections measured at backward angles for 81- [32,33] and 88-keV [34] incident photon energies for Ta, Au, and Pb, and Au, Pb, and Bi (having a K -shell binding energy close to the incident photon energy), respectively, exhibit moderate differences from the S -matrix values. However, differences with the MF+ASF values are found to be considerably large. In general, poor agreement with the MF+ASF cross sections can be due to inaccurate predictions of ASF's. Also, the ASF's may have an angular dependence. Indeed, comparison of S -matrix and MF+ASF calculations indicate that the ASF's are angle dependent at energies well above the K -shell binding energies and at large angles [17]. Theoretical modeling to include the angular dependence of ASF's is not yet established. Thorough scattering measurements at different angles, particularly at large ones, will be helpful in understanding the salient features of anomalous scattering.

IV. CONCLUSIONS

Elastic-scattering cross sections for 59.54-keV photons by 42 elements with $12 \leq Z \leq 92$ have been measured at an angle of 121° . The measured cross sections are found to be enormously lower than the MF values, for the elements with a K -shell electron binding energy in the vicinity of the incident photon energy. These deviations are significantly reduced when MF's are corrected for angle-independent anomalous scattering factors. The S -matrix and MF+ASF values repre-

sent the trend of the measured data over the whole atomic region under investigation. The S -matrix values, in general, exhibit better agreement. The measured cross sections for the low- Z elements (below $Z=26$) agree well with the MF+ASF and S -matrix values. Thereafter, these theoretical cross sections deviate from the measured values, and are, on the average, higher by 17% and 24%, respectively, for the elements with $39 \leq Z \leq 67$. In case of Er, with a K -shell binding energy ($E_K=57.486$ keV) close to the incident photon energy, the MF+ASF value agrees with the measured one, and the S -matrix value is lower by 12%. For the elements with $Z \geq 70$, the S -matrix values are moderately higher by 10% than the measured ones while the MF+ASF values are higher by 19%. Fairly good agreement of the present measured cross sections with the theoretical values [8,17] for low- Z elements infers that the method adopted for a determination of the incident photon intensity, detector efficiency, and other geometrical factors ($I_0 G \epsilon_{el}$ factor) is satisfactory. The present work provides a reliable comparison of the experimental results with the theoretical results, as it covers a large number of elements over the wide atomic region $12 \leq Z \leq 92$.

ACKNOWLEDGMENTS

The authors are thankful to Dr. Lynn Kissel from the Lawrence Livermore National Laboratory, U.S. for providing the scattering cross-section data based on S -matrix calculations. Financial support from the University Grants Commission (UGC), New Delhi, under the Centre of Advance Study Programme, and the Department of Science and Technology (DST), New Delhi, is acknowledged.

-
- [1] L. Kissel and R. H. Pratt, in *Atomic Inner Shell Physics*, edited by B. Crasemann (Plenum, New York, 1985), Chap. 14.
- [2] J. Karle, *Phys. Today* **42**(6), 22 (1989).
- [3] R. Cesareo, A. L. Hanson, G. E. Gigante, L. J. Pedraza, and S. Q. G. Mahataboally, *Phys. Rep.* **213**, 117 (1992).
- [4] R. Cesareo, in *Nuclear Analytical Techniques in Medicine*, edited by R. Cesareo (Elsevier, Amsterdam, 1988), p. 121.
- [5] M. F. Araujo, P. Van. Espen, and R. Van Grieken, *X-Ray Spectrom.* **19**, 29 (1990).
- [6] J. H. Hubbell, W. J. Veigele, E. A. Briggs, R. T. Brown, D. T. Cromer, and R. J. Howerton, *J. Phys. Chem. Ref. Data* **4**, 471 (1975); **6**, 615(E) (1977).
- [7] J. H. Hubbell and I. Øverbrø, *J. Phys. Chem. Ref. Data* **8**, 69 (1979).
- [8] D. Schaupp, M. Schumacher, F. Smend, P. Rullhusen, and J. H. Hubbell, *J. Phys. Chem. Ref. Data* **12**, 467 (1983).
- [9] L. Kissel, R. H. Pratt, and S. C. Roy, *Phys. Rev. A* **22**, 1970 (1980).
- [10] P. P. Kane, L. Kissel, R. H. Pratt, and S. C. Roy, *Phys. Rep.* **140**, 75 (1986).
- [11] B. Zhou, R. H. Pratt, S. C. Roy, and L. Kissel, *Phys. Scr.* **41**, 495 (1990).
- [12] L. Kissel, B. Zhou, S. C. Roy, S. K. Sen Gupta, and R. H. Pratt, *Acta Crystallogr., Sect. A: Found. Crystallogr.* **51**, 271 (1995).
- [13] S. C. Roy, B. Zhou, L. Kissel, and R. H. Pratt, *Indian J. Phys. B* **67**, 481 (1993).
- [14] D. T. Cromer and D. A. Liberman, *Acta Crystallogr., Sect. A: Found. Crystallogr.* **37**, 267 (1981).
- [15] L. Kissel and R. H. Pratt, *Acta Crystallogr., Sect. A: Found. Crystallogr.* **46**, 170 (1990).
- [16] B. L. Henke, E. M. Gullikson, and J. C. Davis, *At. Data Nucl. Data Tables* **54**, 181 (1993).
- [17] L. Kissel (private communication).
- [18] M. Schumacher and A. Stoffregen, *Z. Phys. A* **283**, 15 (1977).
- [19] J. Eichler and S. deBarros, *Phys. Rev. A* **32**, 789 (1985).
- [20] F. Smend and H. Czerwinski, *Z. Phys. D* **1**, 139 (1986).
- [21] S. S. Nandi, R. Dutta, and N. Chaudhuri, *J. Phys. B* **20**, 4027 (1987).
- [22] K. M. Varier and M. P. Unnikrishnan, *Nucl. Instrum. Methods Phys. Res. A* **280**, 428 (1989).
- [23] E. Casnati, C. Baraldi, and A. Tartari, *Phys. Rev. A* **42**, 2627 (1990).
- [24] S. K. Ghose, M. Ghose, S. S. Nandi, A. C. Nandi, and N. Choudhri, *Phys. Rev. A* **41**, 5869 (1990).
- [25] N. G. Nayak, K. Siddappa, K. M. Balakrishna, and N. Lingappa, *Phys. Rev. A* **45**, 4490 (1992).
- [26] S. Puri, B. Chand, D. Mehta, M. L. Garg, N. Singh, and P. N. Trehan, *Nucl. Instrum. Methods Phys. Res. B* **111**, 209 (1996).

- [27] J. S. Shahi, S. Puri, D. Mehta, M. L. Garg, N. Singh, and P. N. Trehan, *Phys. Rev. A* **55**, 209 (1997).
- [28] E. Browne and R. B. Firestone, in *Table of Radioactive Isotopes*, edited by V. S. Shirley (Wiley, New York, 1986).
- [29] J. Singh, R. Singh, D. Mehta, N. Singh, and P. N. Trehan, in *Proceedings of the DAE Symposium on Nuclear Physics* [*Nucl. Phys. B* **37**, 455 (1995)].
- [30] E. Storm and H. I. Israel, *Nucl. Data, Sect. A* **7**, 565 (1970).
- [31] S. Puri, B. Chand, D. Mehta, M. L. Garg, N. Singh, and P. N. Trehan, *At. Data Nucl. Data Tables* **61**, 289 (1995).
- [32] G. Basavaraju, P. P. Kane, L. Kissel, and R. H. Pratt, *Pramana, J. Phys.* **44**, 545 (1995).
- [33] G. Basavaraju, P. P. Kane, L. Kissel, and R. H. Pratt, *Phys. Rev. A* **49**, 3664 (1994).
- [34] G. Basavaraju, P. P. Kane, S. M. Lad, L. Kissel, and R. H. Pratt, *Phys. Rev. A* **51**, 2608 (1995).